Purification and characterization of chaperone-active clusterin

Travis Rilea

Department of Pharmacology & Therapeutics

McGill University, Montreal

April 2017

A thesis submitted to McGill University in partial fulfillment of the requirements of the degree of Master of Science in Pharmacology & Therapeutics

Table of Contents

Figures

Abbreviations

AD	Alzheimer Disease
APP	Amyloid precursor protein
BSA	Bovine serum albumin
FBS	Fetal bovine serum
HEK293	Human embryonic kidney 293
IP	Immunoprecipitation
kDa	Kilodaltons
MALDI	Matrix-assisted laser desorption/ionization
MES	2-(N-morpholino)ethanesulfonic acid
MS	Mass spectrometry
PBS	Phosphate buffered saline
SPR	Surface Plasmon Resonance
SDS- PAGE	Sodium dodecyl sulfate – polyacrylamide gel electrophoresis
TBS	Tris buffered saline
Tris	Tris(hydroxymethyl)aminomethane

Abstract

Alzheimer Disease is one of the largest health care challenges facing our world and is projected to become an even greater burden, especially as there is currently no effective treatment or cure for the disease. Although the exact mechanisms involved in the pathogenesis of the disease are still unclear, it is hypothesized that accumulation of amyloid-β is the main driver of the disease. Amyloid-driven changes in brain physiology occur decades before the emergence of the first detectable symptoms.

Clusterin has been identified by genome-wide association studies as a potential risk factor for AD, and studies have shown that clusterin can interact with amyloid-β to prevent aggregation, which is a process widely associated with the disease.

Here we developed key methods and tools for the further investigation of clusterin's role in Alzheimer Disease. We obtained a monoclonal antibody for clusterin and were able to produce a sufficient amount of antibody to create an immunoaffinity column for the purification of recombinant clusterin. Analysis of the final product showed that we produced pure clusterin, while assessment of the chaperone activity demonstrated that it retained its biological activity through the purification process. We also expanded on previously developed surface plasmon resonance techniques to enable the analysis of clusterin-lipid interactions, which had previously been found increased in AD.

Taken together, the techniques developed by this project provide the foundation for an in-depth investigation of the role of clusterin in health and in Alzheimer Disease.

Résumé

La maladie d'Alzheimer est un des plus grands défis qui face notre système de soins de santé, qui est aggravé par le fait que aucun traitement n'existe. Même si des mécanismes exacts qui causent la maladie ne sont La maladie d'Alzheimer est un des plus grands défis auxquels fait face notre système de soins de santé, et qui est aggravé par le fait qu'aucun traitement n'existe. Même si les mécanismes exacts qui causent la maladie ne sont pas clair, l'hypothèse la plus établie est que la suraccumulation du peptide bêta amyloïde est le facteur principal pour la pathogenèse de la maladie, et que ces changements peuvent exister des décennies avant l'apparition des premiers symptômes détectables. Clusterin a été identifié par des études d'association à l'échelle du génome comme un facteur de risque potentiel pour la maladie d'Alzheimer. D'autres études ont démontré que la clusterin peut interagir avec des peptides β-amyloïdes et les empêche d'agréger. Comme l'agrégation de ces peptides est un processus associé au développement de la maladie il y a une possibilité réelle que la clusterin pourrait être impliqué dans la maladie. Ici, nous avons mis au point des méthodes et outils importants pour continuer l'étude du rôle de clusterin dans la maladie Alzheimer. Nous avons exprimé et isolé un anticorps contre la clusterin, et avons produit une quantité suffisante pour créer une colonne d'immuno-affinité pour purifié la clusterin recombinante. L'analyse du produit final de la purification a révélé que nous avons produit une clusterin pure, et l'évaluation de l'activité chaperonne a démontré qu'elle avait conservé son activité biologique à travers le processus de purification. Nous avons aussi amélioré des méthodes de résonance de surface plasmonique pour l'analyse des interactions clusterin-lipides, qui ont déjà été démontré comme étant affectées chez les patients atteints de la maladie d'Alzheimer. Prisent ensembles, les techniques développées

par ce projet fournissent la fondation pour une étude approfondie sur le rôle de clusterin dans la maladie d'Alzheimer.

Acknowledgements

Many people have contributed to the realization of this project as well as my growth as a student and individual over the course of my time at McGill and it would be impossible to list them all, however I would like to thank some of the particularly key people.

First of all I would like to thank my supervisor, Professor Multhaup, for the opportunity to work in his laboratory, for funding my work on this project, and for his support and advice throughout it.

I would next like to thank Mark Hancock from the Department of Pharmacology SPR/MS facility, whose assistance in designing and performing the SPR and MALDI-MS experiments in this thesis was invaluable.

Thanks to Shireen for her input on the overall direction of my project, specific advice on experimental methods and design, and last of all (but certainly not least) for her plentiful words of encouragement which helped me get through the lows of endless troubleshooting.

Thanks also to my advisory committee for their insight, support, and helpful suggestions on my project.

My time at McGill wouldn't have been the same without the great atmosphere on the first floor Bellini, and I thank Shaon, Phoebe, Filip, Can, Corvin, Jana, Meng, Nancy, as well as the others I don't have space to list for contributing to an amazing working atmosphere.

Finally, my thanks go out to my Mom, Dad, and brother: for their unconditional support, for always being there to prove a listening ear, and for believing in me throughout it all. You mean more to me than words can express.

Preface & Contribution of Authors

The work presented in this thesis builds on the SPR-MS experiments performed by a previous PhD student in our lab, Veit Althoff, who established the initial methods for studying lipid binding interactions via surface plasmon resonance and discovered the altered lipid binding of clusterin in AD patient cerebrospinal fluid. Mark Hancock performed the ISD sequencing of clusterin. Mark and I collaboratively performed the remaining SPR and mass spectrometry experiments. I performed and analyzed all other experiments, with supervision and overall project design from Dr. Hossain and Dr. Multhaup.

Introduction

Alzheimer Disease (AD)

Alzheimer Disease (AD) is the leading cause of dementia in the western world (1) and places an ever-increasing burden on the health care systems of developed nations. A 2006 model predicted that the number of cases would triple from the then-current 26.6 million to nearly 80 million by 2050 (2). In the United States alone there are currently over 5 million cases of AD (3), making it the 6th leading cause of death and incurring an estimated $100 billion in care costs (4). This cost is amplified by the fact that there is currently no effective cure, treatment, or even early diagnostic tool to help fight the disease, making long-term care the only option. The development of any one of these is urgently needed to combat the looming burden to society that this disease will impose as the world's population ages.

While the etiology of AD remains unclear, it is typically thought to be defined by two major processes: the deposition of amyloid plaques (5) and emergence of neurofibrillary tangles comprised of the cytoskeletal protein tau (6). While tau pathology undoubtedly plays an important role in the disease, current leading theories of the disease progression focus on the contributions of the amyloid plaques and the amyloid-β peptides.

The Amyloid Hypothesis

Amyloid-β (Aβ) peptides are a family of peptides produced from the sequential cleavage of the amyloid precursor protein (APP) by two membrane-bound secretases, the β and gamma secretases (7). This cleavage process results in the generation of various peptide species, of which the most studied are the 40- and 42-amino acid long forms, typically referred to as amyloid-β 40 (Aβ_{40}) and amyloid-β 42 (Aβ_{42}) respectively.

Although the aggregation of the amyloid-β peptides into macroscopic plaques in the brain is one of the most commonly recognized hallmarks of AD (8), current evidence suggests that the pathogenic effect of these peptides occurs at an earlier stage, specifically when they come together to form "low-n" oligomers (9), which are still soluble in the extracellular space. The Aβ_{42} peptide in particular seems to be the driving species behind cellular toxicity and pathogenesis (10), as it has been shown to be much more prone to aggregation (11) and to exhibit much stronger toxic effects *in-vitro* than the Aβ_{40} form (12). Although the key role these peptides play in the disease seems to be quite well-established we still lack mechanistic insight into the pathways through which amyloid peptides induce toxicity and research into potential interaction partners and toxicity mechanisms is expected to yield new insight into the pathology of AD.

Forms of Alzheimer Disease

Two overarching forms of AD are recognized: familial (also known as early-onset) AD (FAD) which results from inherited mutations in one of the key proteins involved in the generation of amyloid-β (13), and non-familial (or late-onset) AD which has more diverse and largely unknown causes (14). FAD accounts for approximately 1% of all cases (15) and arises mostly from mutations of the APP gene, or the presenillin-1 and presenillin-2 subunits of the gamma secretase (16). Non-familial AD accounts for the vast majority of cases, with 95% of patients having this form of the disease (17) which, unfortunately, is much less well-understood than the familial form of the disease. Although there are no direct genetic mechanisms at play in non-familial AD there are several gene variants which have been identified through genome-wide association studies (GWAS) as imparting an increased risk for AD to individuals which carry them (18). One such gene variant is found in the CLU gene, which encodes for the protein clusterin (19).

Clusterin

Clusterin is a secreted glycoprotein that is ubiquitously expressed throughout the body and has diverse roles in many physiological functions (20). It was first isolated from ram rete testis fluid where it was observed to promote clustering of Sertoli cells, giving rise to the current widely-used name (21). Further studies revealed that this protein was the same as several previously identified proteins with a wide array of names, tissues of origin, and proposed functions (22) including lipid transport and metabolism (23), cell-cell adhesion (24), extracellular protein quality control (25), inhibition of cell lysis by the complement system (26), sperm maturation (27), and inhibition of apoptosis (28).

The gene for clusterin is located on chromosome 8 and contains 9 exons (29), which give rise to mRNAs for the various isoforms through differential splicing (30). The major form of clusterin is first translated into the ER as a 449-amino acid pre-pro-protein which is then cleaved to remove the secretory signal sequence and extensively glycosylated at six *N*-linked glycosylation sites (31). The proprotein is then cleaved again to generate α and β chains which remain linked through five disulfide bridges to form the mature protein. Clusterin is predicted to contain two coiled-coil α helices and three amphipathic α helix domains, which likely act as molten globule domains (32) and are hypothesized to be key domains for chaperone activity (33). Increases in clusterin expression have been shown to occur in a number of pathological processes including myocardial infarction (34), ischemic or pressure-induced kidney damage (35), and neurodegeneration, including Alzheimer disease (36). Despite the numerous processes clusterin appears to be involved in, the most likely role for this protein in the context of AD is as an extracellular chaperone.

Chaperone Proteins

Chaperone proteins are a class of proteins which stabilize partially translated or denatured proteins by binding to exposed hydrophobic regions, preventing the formation of insoluble and potentially toxic aggregates (37). Some chaperones, known as folding-helper chaperones, are then able to induce the protein to fold correctly in an ATP-dependent (Heat shock protein 90 (Hsp90), Hsp70, Hsp60) (38) or ATP-independent (calnexin and calreticulin) (39) process, while other chaperones merely stabilize the misfolded protein until a folding-helper chaperone is available, or until the protein is flagged for degradation (40).

Many of these proteins are found at sites of protein synthesis in the cytosol and endoplasmic reticulum, where they assist in the folding of newly synthesized polypeptides or facilitate the refolding of proteins which have been denatured by some insult (41), however there are also two known extracellular chaperones, clusterin and haptoglobin, which provide this same quality control for extracellular proteins (42).

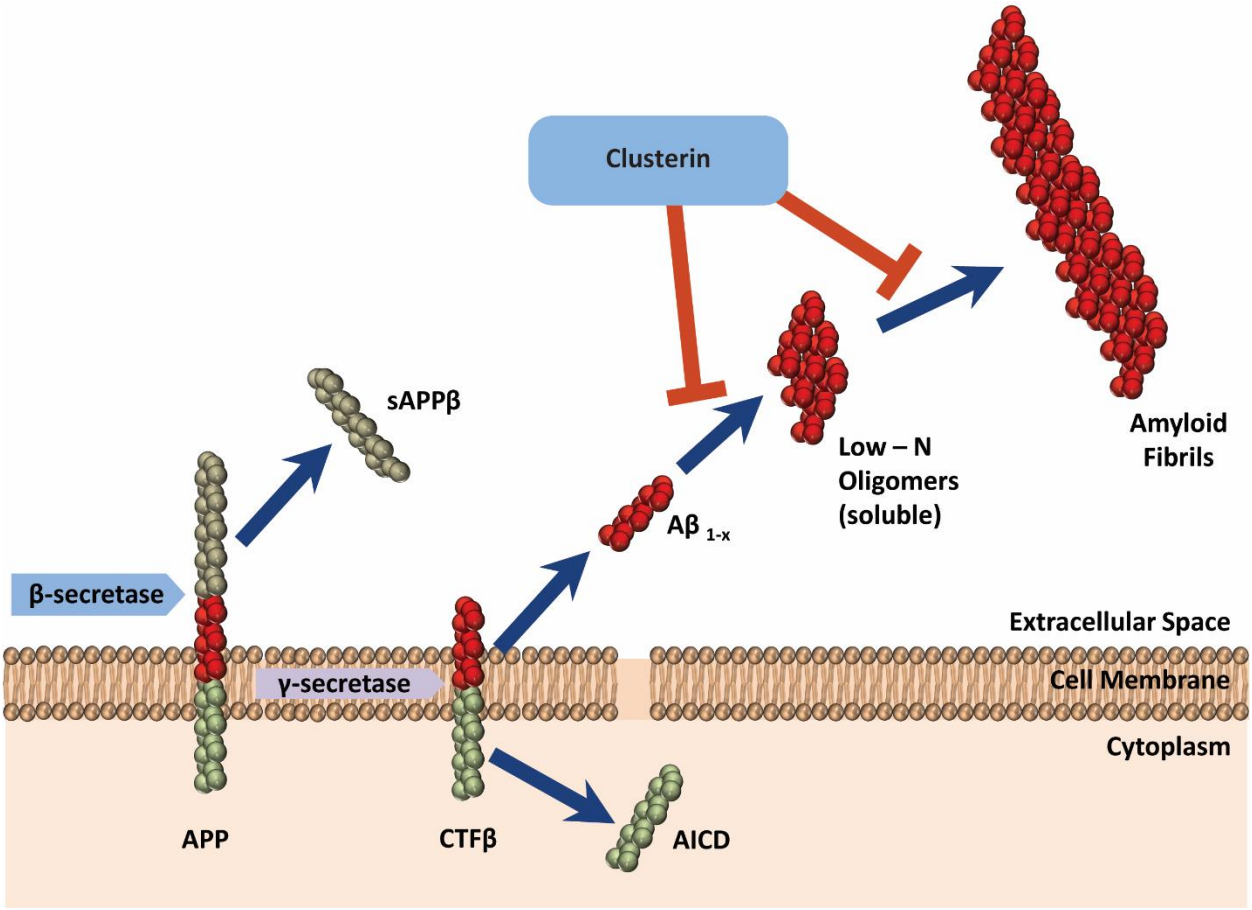

Figure 1. Possible role of clusterin in Alzheimer Disease. Amyloid-β is generated by the sequential cleavage of amyloid precursor protein, which releases the peptides into the extracellular space where they aggregate into soluble oligomers and eventually into larger fibrils that go on to form amyloid plaques. Clusterin is proposed to interfere with this process at two points: the aggregation of individual peptides to form low-n oligomers, and the generation of fibrils from these smaller oligomers.

Role of Clusterin in AD

As an extracellular chaperone, clusterin has a demonstrated ability to bind intermediate folding states of proteins, stabilizing them into soluble complexes and preventing the formation of potentially toxic insoluble aggregates (43). Given that the amyloid hypothesis of AD posits that the progression of the disease is driven by the accumulation of insoluble, hydrophobic peptide aggregates, the potential for clusterin to act as a chaperone and interact or interfere with the process of amyloid-β peptide oligomerization and fibrilization seems intuitive. Confirming this, studies on the specific interactions between clusterin and amyloid peptides have shown that clusterin is able to interact with a wide range of aggregation states of Aβ peptides (Figure 1) (44), that it prevents the formation of insoluble fibrils (45), and reduces levels of low-n oligomers in-vitro (46).

While the implication of the CLU gene as an AD risk factor by GWAS and compelling evidence in the literature for a direct interaction between clusterin and Aβ peptides point towards a role for clusterin in AD, the specific mechanisms through which clusterin may play a role remain unclear. One piece of this puzzle may be provided by as-yet unpublished data from our laboratory. We used surface plasmon resonance (SPR) to analyze the lipid binding capacity of cerebrospinal fluid (CSF) from both AD patients and healthy controls. It was found that injecting CSF from AD patients over a lipid surface produced a greater binding response than did non-AD CSF, and mass spectrometry analysis of the bound proteins found that the major protein behind this change was clusterin. Further preliminary experiments did not find increased levels of clusterin in CSF from AD patients which suggests that there may be some alteration to the function of clusterin in AD, however there are as-yet unanswered questions regarding the role of this protein in AD.

Firstly, is the alteration in clusterin's function a result of other aspects of the AD pathology, such as amyloid β accumulation, or do changes to clusterin predate the emergence of the disease? If the latter is true then analysis of clusterin function could serve as a biomarker to detect individuals who are likely to develop the disease long before the appearance of cognitive symptoms or even amyloid-β plaques. In order to answer this question satisfactorily a thorough understanding of the exact alterations that occur to clusterin in AD, and the mechanism through which they arise is required. Determining the mechanisms at play requires the application of biochemical techniques such as mutational analysis to understand the impact of AD-linked polymorphisms on the function of clusterin, and ideally would include structural data to draw a better picture of the role that this protein has in AD.

Another question is whether clusterin interaction with amyloid-β has functional consequences for progression of AD pathology in-vivo. Even if changes to the activity of clusterin are found to be caused by interaction with amyloid-β and thus cannot be used as a viable biomarker, clusterin could still play an important role in the progression of the disease. For instance, if the chaperone activity of clusterin proves to be protective against amyloid-β induced toxicity this finding could open new avenues for the development of therapeutic strategies based on sequestering or otherwise neutralizing amyloid-β.

Answers to these questions and further insight into the role clusterin may play in AD can be gained by using techniques such as mass spectrometry, surface plasmon resonance, mutagenesis experiments, and *in-vitro* cell viability assays, however the precursor to performing any such experiments is the generation of sufficient quantities of recombinant clusterin for analysis. In addition, the experimental techniques used in the pilot SPR studies which first

revealed a potential difference in clusterin from AD patients and that from healthy controls required further development in order to expand on these previous findings.

Production of Recombinant Clusterin

To date attempts to produce recombinant clusterin in the literature have met with limited success (47). Due to the proteolytic processing and high degree of glycosylation required to generate the mature form of clusterin, the use of bacterial expression systems to produce a recombinant protein which retains the characteristics of native clusterin is not possible. Despite this, previous attempts have been made to express clusterin in bacterial cells (48), as it had been shown that clusterin retained chaperone activity after enzymatic de-glycosylation (49) and it was not known if proteolytic processing and the resulting α/β chain structure was required for the chaperone activity of clusterin. Unfortunately, clusterin expressed in bacteria was found to be insoluble as aggregates in inclusion bodies within bacteria and did not show chaperone activity after solubilization and purification (50). Other attempts to express clusterin using yeast systems generated a product that was proteolytically degraded (51) while expression of clusterin in insect cell lines resulted in a product which was not cleaved into the α- and β-chains (52).

One study has been published which used a purification protocol for clusterin expressed in human embryonic kidney cells (50), which appeared to be properly cleaved and glycosylated. Critically, the chaperone activity of the purified product was demonstrated and the recombinant protein is regarded as a benchmark for the quality of the recombinant product in comparison to clusterin purified from human plasma.

Objectives

In this thesis we established a purification method based on published data by Dabbs and Wilson (50) for the generation of pure, chaperone active clusterin. The clusterin produced by this method was characterized by mass spectrometry and Western blotting to determine its purity, while the physiological activity of purified clusterin was measured using a protein aggregation assay. Additionally, we expanded on the previously developed SPR techniques for the analysis of clusterin-lipid binding by developing a non-interactive control surface in order to further investigate the role this interaction may have in Alzheimer Disease.

Results

Production of G7 anti-Clusterin antibody

In order to produce the immunoaffinity column which we planned to use for the first step of our clusterin purification strategy we first aimed to produce ~25 mg of anti-clusterin antibody to achieve the recommended minimum antibody concentration of 5 mg/mL for a 5 mL affinity column. In order to produce this large amount of antibody we used a hybridoma cell line which secretes a monoclonal antibody specific for Clusterin (designated G7), obtained from the lab of Mark Wilson. After being conditioned by confluent G7 hybridoma cultures, harvested media containing the antibody was pumped over a protein G column to purify the antibody. An initial bulk A280 absorbance was observed, as the absorbance of various protein components of the loaded media created a plateau of 2600 mAU. Washing the column with 25 mL of PBS did not release any material which absorbed at 280 nm. Elution of the antibody was performed with 100 mM glycine (pH 2.7) and resulted in a single A280 absorbance peak. The maximum absorbance of this peak varied with yield and was used to provide an initial estimate of the total amount of antibody purified. The supernatant and flow-through was analyzed via Western blotting to verify that a maximum yield of antibody was purified from the supernatant, and to show that the binding capacity was sufficient to capture all antibody from the harvested media.

A

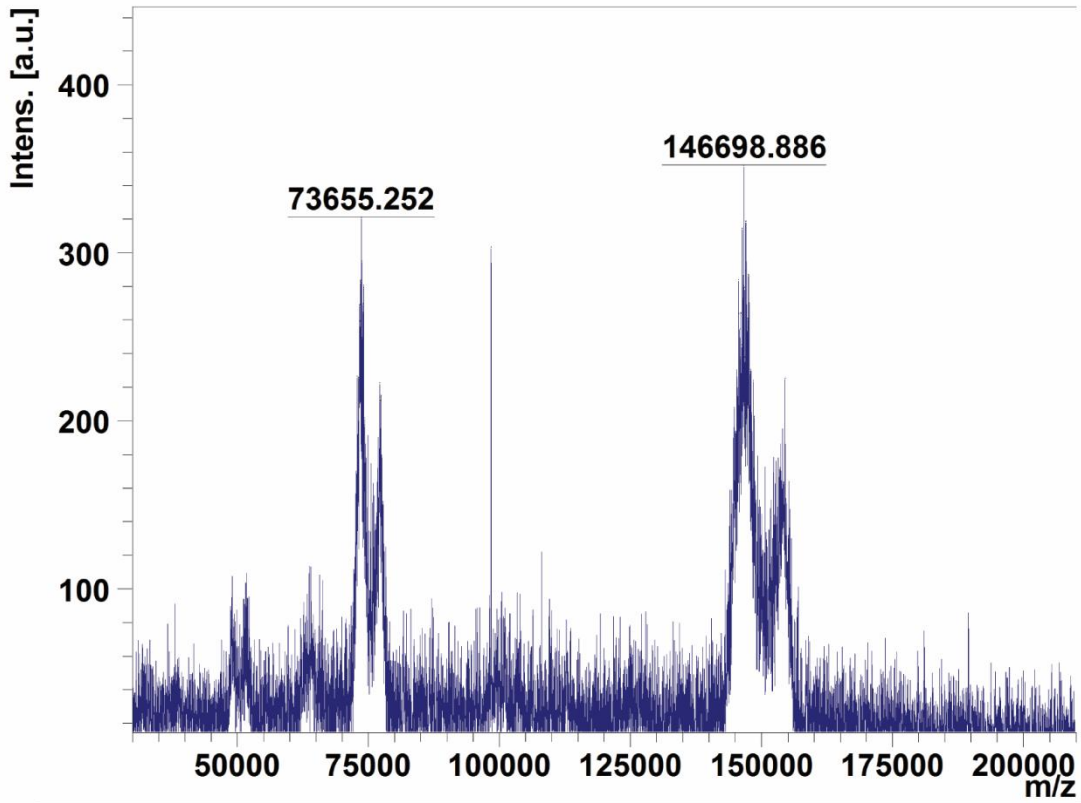

B

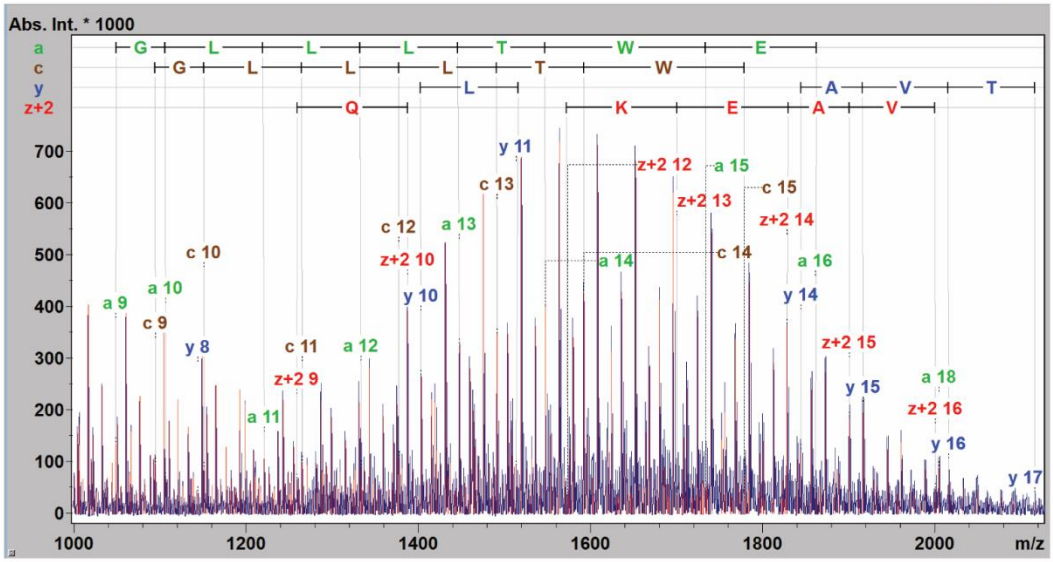

C

MMKTLLLFVGLLLTWESGQVLGDQTVSDNELQEMSNQGSKYVNKEIQNAVNGVKQIKTLIEKTNEERKTLLSNLEEAK

KKKEDALNETRESETKLKELPGVCNETMMALWEECKPCLKQTCMKFYARVCRSGSGLVGRQLEEFLNQSSPFYFWMN

GDRIDSLLENDRQQTHMLDVMQDHFSRASSIIDELFQDRFFTREPQDTYHYLPFSLPHRRPHFFFPKSRIVRSLMPFSPY

EPLNFHAMFQPFLEMIHEAQQAMDIHFHSPAFQHPPTEFIREGDDDRTVCREIRHNSTGCLRMKDQCDKCREILSVDC

STNNPSQAKLRRELDESLQVAERLTRKYNELLKSYQWKMLNTSSLLEQLNEQFNWVSRLANLTQGEDQYYLRVTTVAS

HTSDSDVPSGVTEVVVKLFDSDPITVTVPVEVSRKNPKFMETVAEKALQEYRKKHREE

Figure 2. MALDI-MS analysis of immunoprecipitated clusterin. An immunoprecipitation was performed using the G7 antibody, protein G-sepharose beads, and supernatant from clusterin expressing HEK293 cells. MALDI-MS analysis of the precipitated material (A) showed two doublet peaks, one with the major component at 73.655 Da and the second with a major component at 146.698 Da. In-source decay sequencing was used to further verify the identity of the protein and was able to detect 8 N-terminal residues and 7 C-terminal residues (B), which are highlighted in the amino acid sequence of human clusterin (C).

Assessment of G7 effectiveness

The effectiveness of the purified G7 antibody was assessed by using it to immunoprecipitate clusterin from the media of HEK293 cells which stably expressed clusterin and secreted it into the media. Analysis of the immunoprecipitation eluent via MALDI-MS (Figure 2) showed a major peak at 73.655 kDa, which is within the range (70-80kDa) of gel electrophoresis-derived apparent molecular weight for monomeric clusterin, as reported in the literature. We also observed an additional major peak at 146.701 kDa. The mass of the second peak is very close to the predicted mass of a clusterin dimer (147 kDa), however, this is also within the predicted mass range for IgG antibodies which is a more likely source for this signal. This indicates that the G7 antibody was also eluted from the protein G beads with the 50% acetic acid elution buffer, as to be expected. However, the antibody would be covalently coupled to the Sepharose material of our immunoaffinity column and thus would not considered to be an issue.

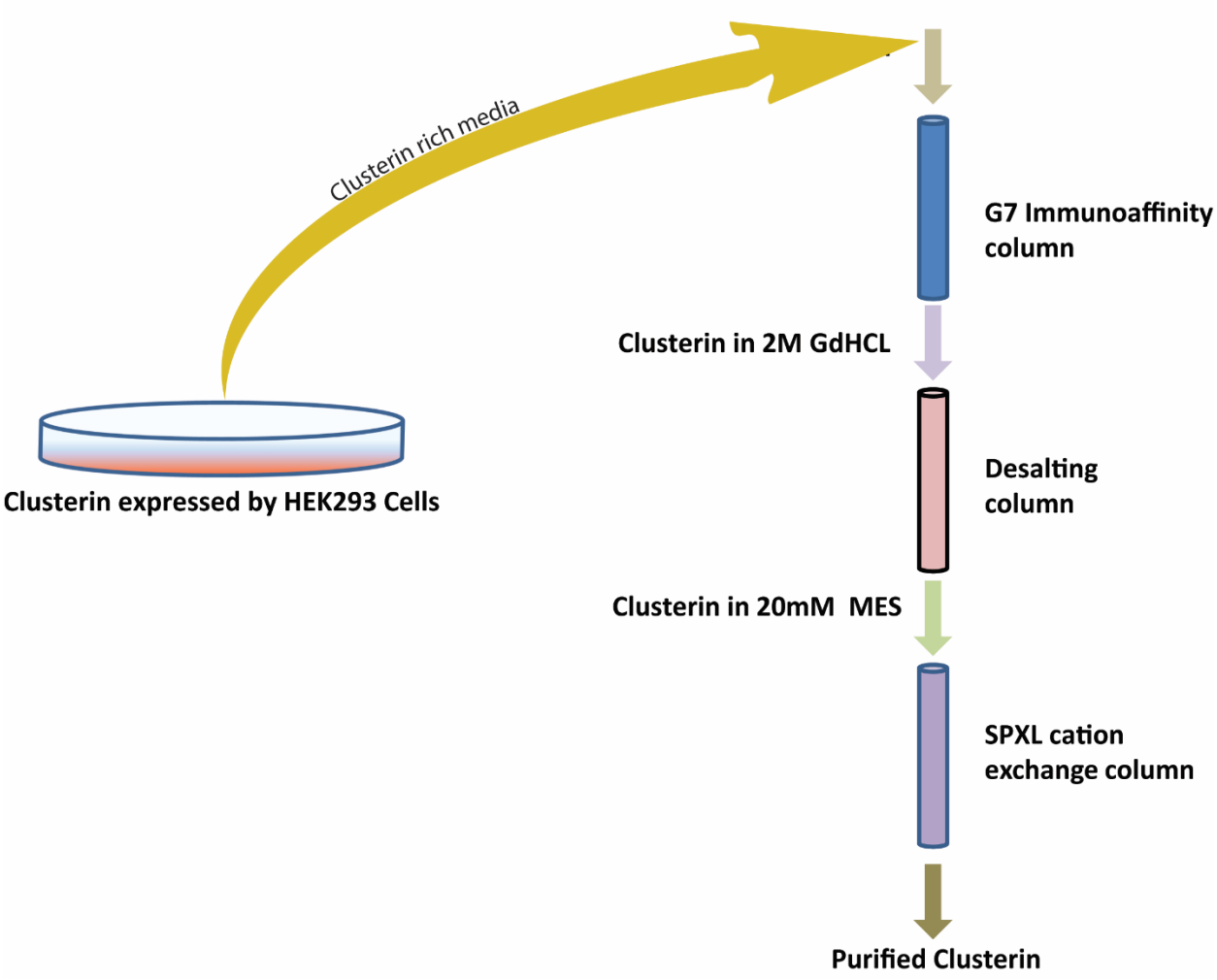

Figure 3. Clusterin purification procedure. Purification of clusterin from HEK293 cell media was achieved in a three-step process. Conditioned media was first pumped over an immunoaffinity column prepared with an anti-clusterin monoclonal antibody. The column was eluted using 2 M guanidine hydrochloride, and the eluate was immediately buffer exchanged into 20 mM MES in preparation for the final cation exchange chromatography step. Clusterin purified from media containing fetal bovine serum (FBS) bound to the column and was eluted using a 0.0 – 1.0 M sodium chloride gradient.

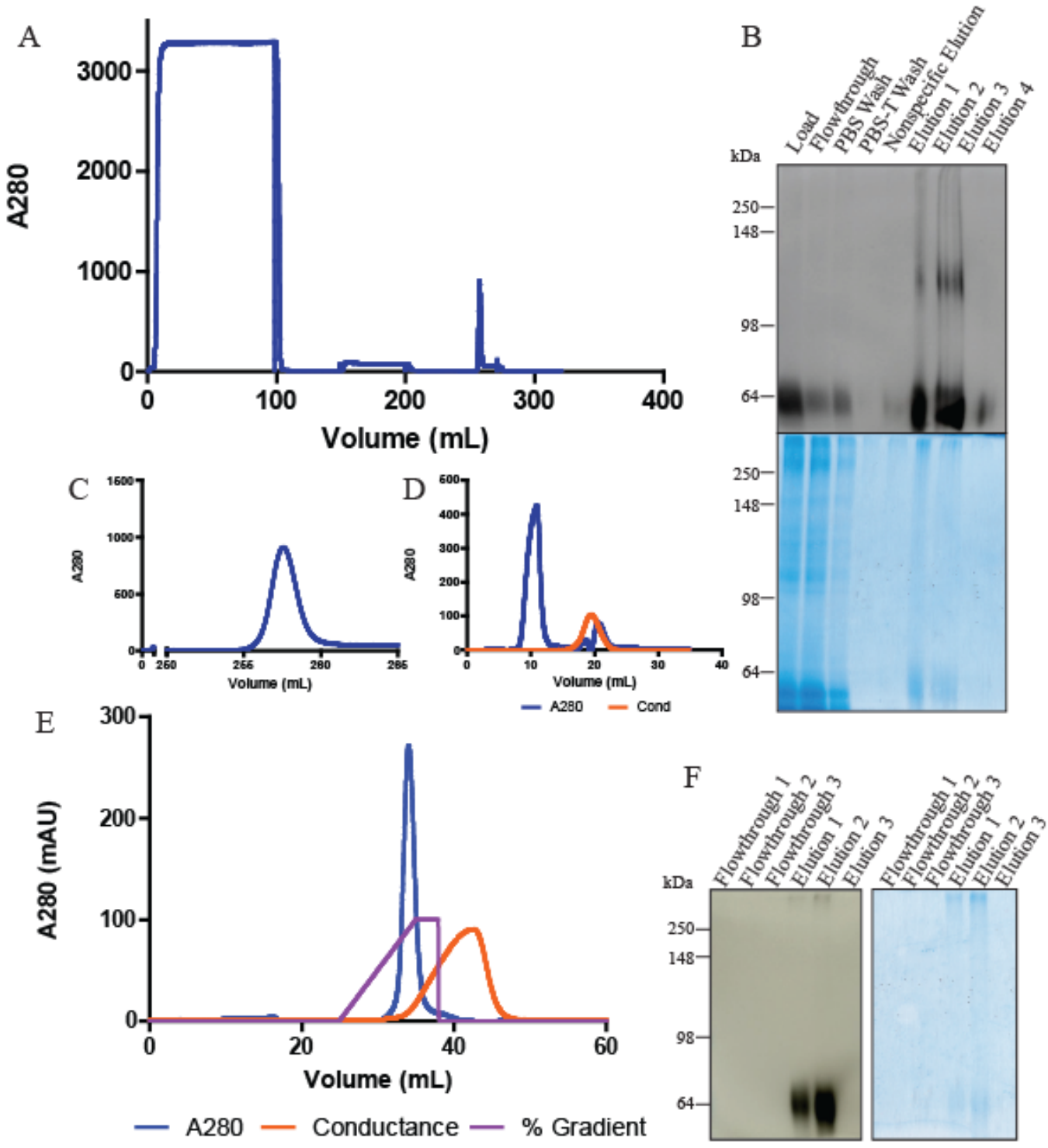
A
A280
3000
2000
1000
0
0
100
200
300
400
Volume (mL)
B
Load
Flowthrough
PBS Wash
PBS-T Wash
Nonspecific Elution
Elution 1
Elution 2
Elution 3
Elution 4
kDa
250
148
98
64
C
A280
Volume (mL)
D
A280
Volume (mL)
A280
Cond
E
A280 (mAU)
Volume (mL)
A280
Conductance
% Gradient
F
Flowthrough 1
Flowthrough 2
Flowthrough 3
Elution 1
Elution 2
Elution 3
kDa
250
148
98
64

Figure 4. Purification of Recombinant clusterin. Media harvested from clusterin-expressing HEK293 cells was first purified by affinity chromatography using a G7 anti-clusterin monoclonal antibody coupled to the column material (A). Initial loading of media produced a large absorbance peak which disapeared as the media loading completed. Elution from the affinity column (C) gerenrated a single peak, the majority of which occupied a volume of 4 mL. Combined Western blot and Coomassie analysis showed some residual clusterin in the flowthrough, but much less than in the initially loaded media. The elution fractions showed a strong signal for clusterin, but very high molecular weight bands can be seen by Coomassie staining which were not immunoreactive. The protein was buffer exchanged into 20 mM MES to prepare for cation exchange and to remove the harsh elution buffer from the sample (D). Complete seperation of the protein, visible as the A280 curve, and the elution buffer, visible as the peak in couductance, was achieved. A final cleanup step was performed using cation exchange chromatography (E)

Purification of recombinant Clusterin

Recombinant clusterin was purified from harvested cell supernatant using a three-step process (Figure 3), with fractions collected from the various stages of the process for assessment via Western blot and Coomassie staining (Figure 4). Western blot analysis of the various affinity chromatograph stages showed a marked reduction of clusterin signal in the flowthrough fraction compared to the initial loading stage. The PBS wash fraction also produced a faint Western blot signal for clusterin, however no further clusterin signal was seen in the immunoblots of fractions from the PBS-T wash or nonspecific elution. Elution from the column produced a single A280 peak with an amplitude of 1000-1400 mAU depending on the yield of each individual run.

Buffer exchange

The eluent from the affinity column was buffer exchanged in order to rapidly remove the recombinant clusterin from the strong denaturing agents present in the elution buffer. Buffer exchange into a MES buffer (Figure 4) showed complete separation of the protein, as assessed by the 280 nm absorbance spectra, and the GdHCl-containing elution buffer, which appears on the chromatograph as an increase in the conductance of the flow through.

Cation Exchange

A cation exchange column was used as a final "polishing" step in the purification process. Clusterin was loaded on the column, and no A280 peak was observed in the flowthrough, indicating that the clusterin present in the loaded material bound to the column (Figure 4). Elution from the column with a 0-1M gradient of sodium chloride yielded a peak in the A280 spectrum which was proven to contain clusterin via Western blot, while a colloidal Coomassie stain showed that no other proteins were present in significant quantities in the eluted fractions.

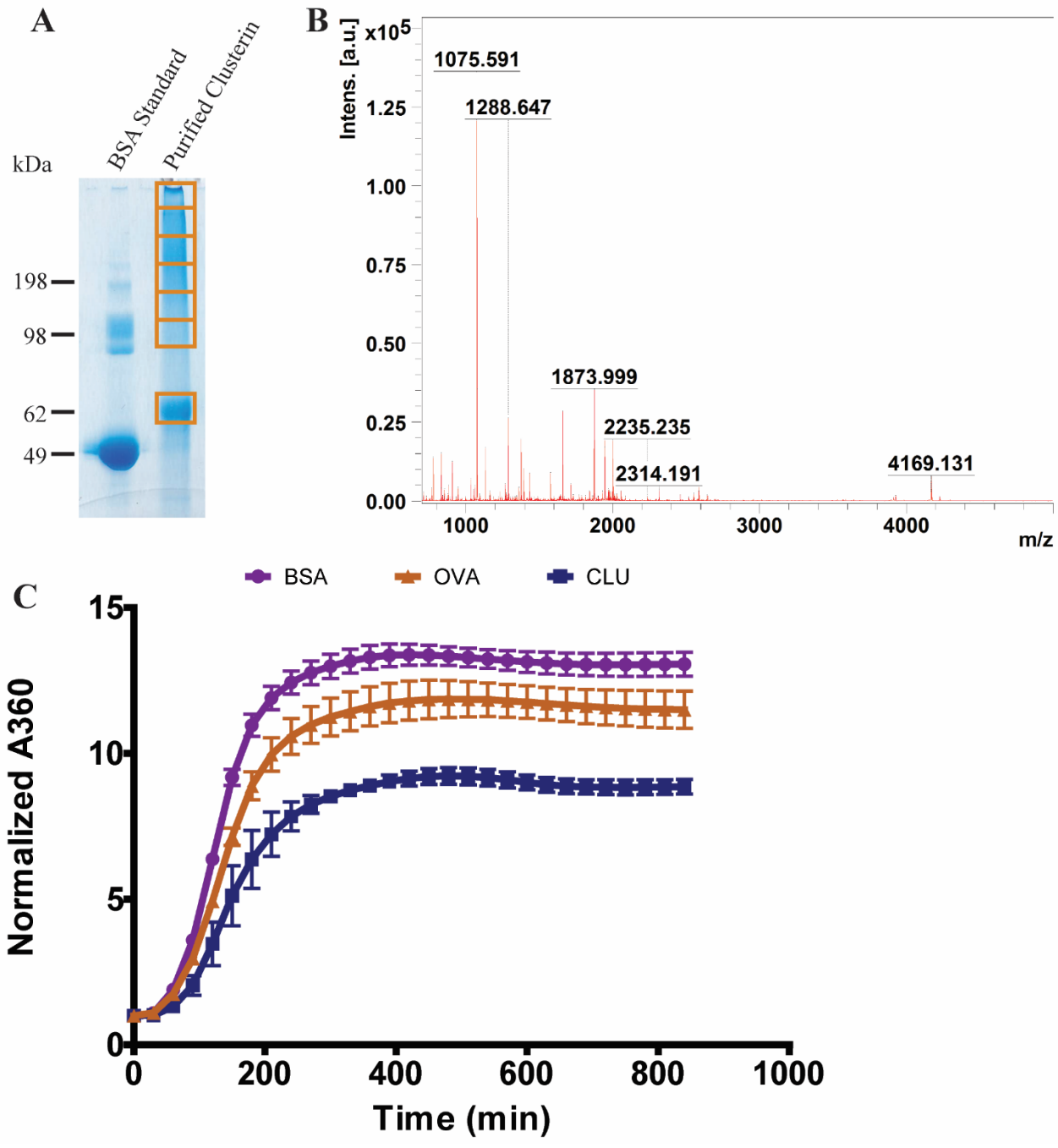
A
BSA Standard
Purified Clusterin
kDa
198
98
62
49
B
x10^5
Intens. [a.u.]
1.25
1.00
0.75
0.50
0.25
0.00
1075.591
1288.647
1873.999
2235.235
2314.191
4169.131
1000
2000
3000
4000
m/z
C
BSA
OVA
CLU
Normalized A360
15
10
5
0
0
200
400
600
800
1000
Time (min)

Figure 5. Characterization of purified clusterin. The identity of clusterin was confirmed by peptide mass fingerprinting. The purified product was first by SDS-PAGE (A) and the bands highlighted in orange were excised and digested with trypsin. The generated peptides were analyzed with MALDI-MS and the mass spectrum from the 75kDa band (B) showed a significant match to human clusterin when compared to the MASCOT database. BSA was included as a control and also produced a significant match with the MASCOT database. The biological activity was verified using the aggregation assay (C) in which BSA (1.5 mg/mL) was incubated alone (BSA), with clusterin (CLU), or with ovalbumin (OVA) in the presence of 2 mM DTT. Clusterin, but not ovalbumin caused a reduction in the A360 relative to the beginning of the experiment, indicating that less protein aggregation occurred.

Characterization of recombinant clusterin

We used a two-pronged approach to verify both the identity and biological activity of the purified recombinant clusterin. We first analyzed the tryptic peptide fingerprint of the eluted protein using MALDI-MS, with BSA as a control protein of known identity to allow verification of the method and subtraction of any background signal (Figure 5). We were able to achieve a significant match for the control BSA protein, which verified the digestion and mass spectrometry methods. When concentrated and then ran on an SDS-PAGE gel the eluted material from the cation exchange column showed a major band at 65kDa, which corresponds with the predicted apparent molecular weight of clusterin, and an indistinct band which stretched from the top of the gel to approximately 100 kDa. The mass spectra of the tryptic peptides after digestion of the 65 kDa band showed a significant match in MASCOT for human clusterin, while the mass spectra obtained from various fractions of the upper band did not produce significant matches for any proteins in the MASCOT database.

The biological activity of purified recombinant clusterin was assessed using a protein aggregation assay (Figure 5). Bovine serum albumin was incubated under mild reducing conditions to induce denaturation and aggregation in the presence of clusterin. We found that co-incubation of clusterin with BSA led to a 40% reduction in the total aggregation (as measured by the absorbance at 360 nm) compared to BSA alone. Incubation of BSA with ovalbumin as a non-chaperone active control protein did not lead to a significant reduction in protein aggregation relative to control levels.

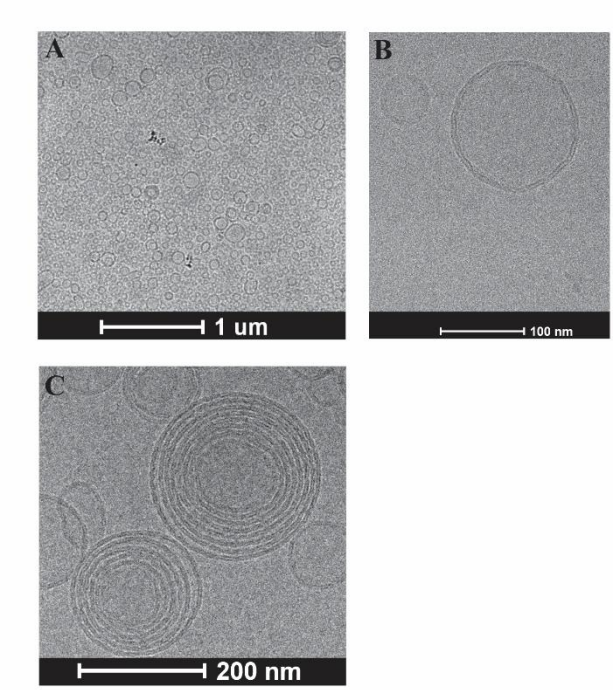

Figure 6. Cryo-Electron Microscopy of liposomes. Liposomes produced via extrusion were imaged using the Titan Kryos electron microscope. When looking at a large-field view (A) the homogeneity of the liposomes was evident, while increased zoom (B) showed that individual liposomes were of the expected size. Some residual multilamellar liposomes (C) remained, but were by far a minor species.

Electron microscopy of liposomes

In order to study the interactions of clusterin with lipid surfaces we used SPR sensor chips with a hydrophobic coating to capture lipids that come into contact with the chip surface. Lipids for this purpose are typically injected in the form of unilamellar liposomes with a diameter between 50 and 100 nanometers. In order to produce liposomes for this purpose we re-hydrated a lipid film in PBS then extruded the resulting multilaminar vesicles to produce unilaminar vesicles of a consistent size. In order to verify the size and lamellarity of the liposomes we imaged the liposomes using cryo-electron microscopy (Figure 6). Imaging of the vesicles showed that nearly all of the liposomes were unilaminar in nature with a limited number of multilaminar liposomes remaining after extrusion. The size of the liposomes was also highly consistent and appeared to be near the expected 100 nm diameter.

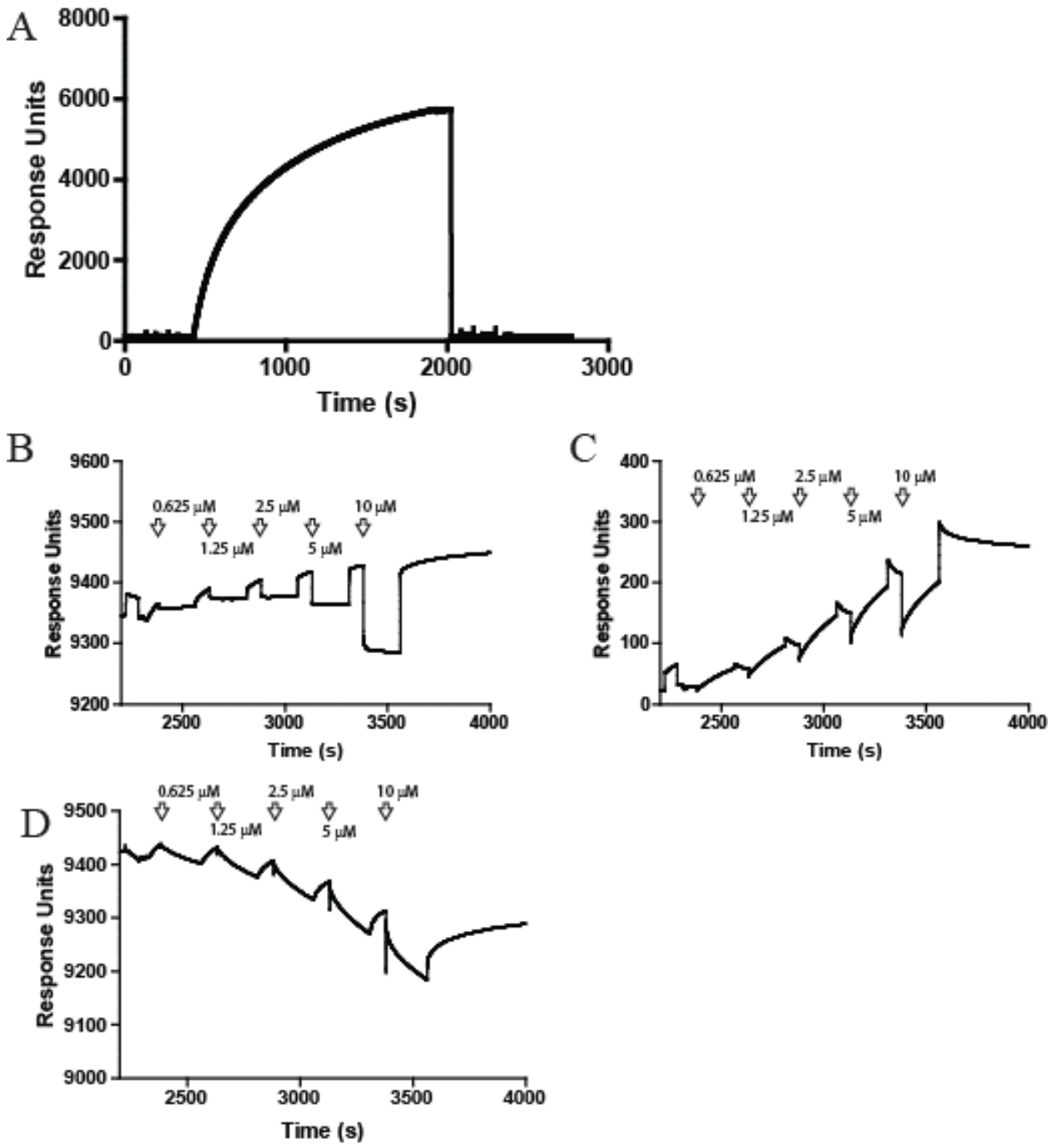
A
Response Units
8000
6000
4000
2000
0
0
1000
2000
3000
Time (s)
B
Response Units
9600
9500
9400
9300
9200
0.625 µM
1.25 µM
2.5 µM
5 µM
10 µM
2500
3000
3500
4000
Time (s)
C
Response Units
400
300
200
100
0
0.625 µM
1.25 µM
2.5 µM
5 µM
10 µM
2500
3000
3500
4000
Time (s)
D
Response Units
9500
9400
9300
9200
9100
9000
0.625 µM
1.25 µM
2.5 µM
5 µM
10 µM
2500
3000
3500
4000
Time (s)

Figure 7. Surface Plasmon Resonance analysis of the binding of Aβ42 to sphingomyelin surface on the L1 sensor chip. Liposomes were injected over the L1 sensor (A) which produced a stable surface. Injection of BSA over both surfaces resulted in binding of a similar amount of material to the reference surface, bringing the subtracted trace of the capture to essentially zero. Injections of Aβ42 over the active (B) and reference (C) surfaces showed binding to the control surface, but not to the reference surface, leading to a negative slope curve in the subtracted trace (D). Arrows indicate the beginning of each injection, with the Aβ42 indicated concentration applied.

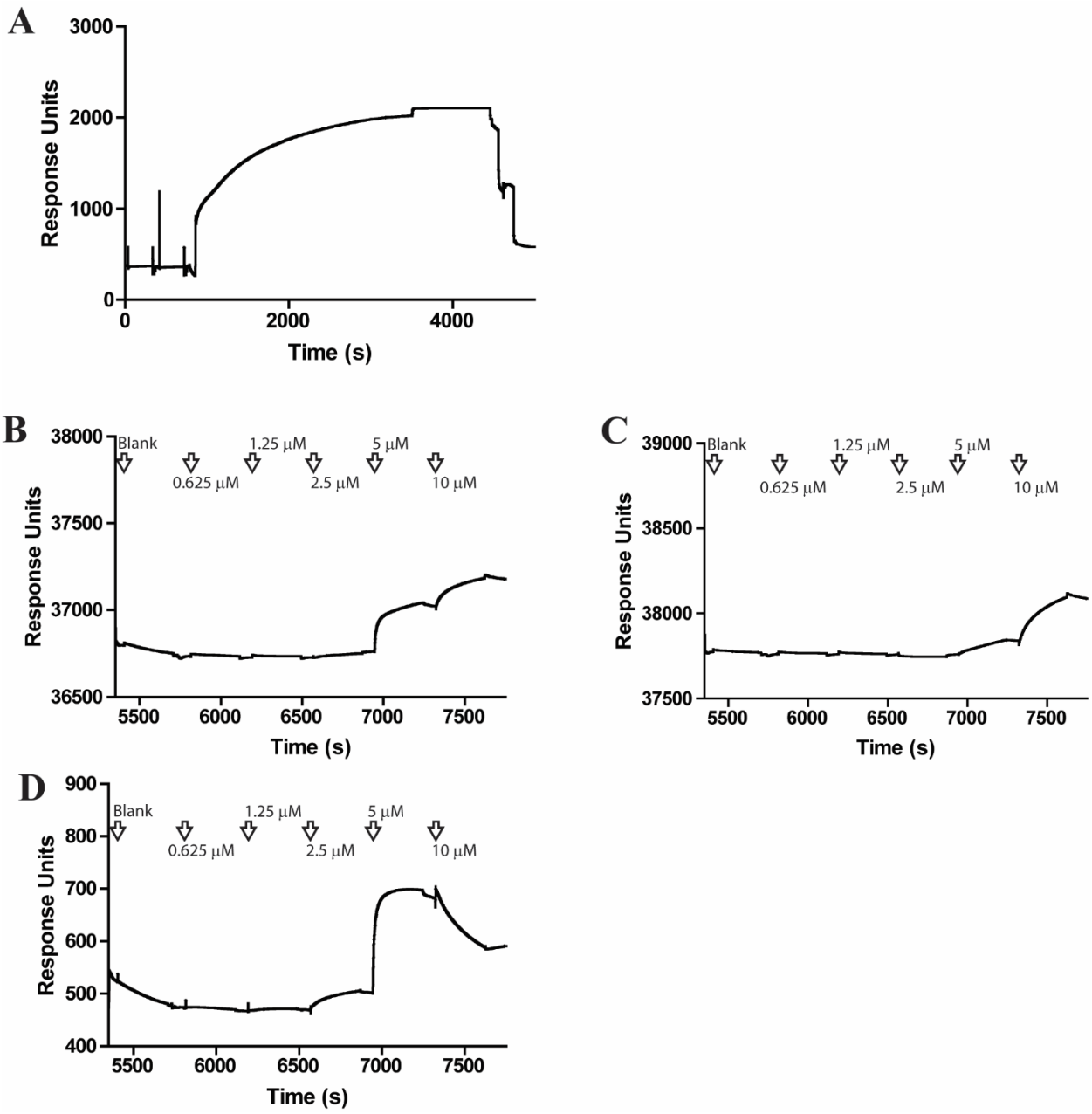
A
Response Units
3000
2000
1000
0
0
2000
4000
Time (s)
B
Response Units
38000
37500
37000
36500
Blank
0.625 µM
1.25 µM
2.5 µM
5 µM
10 µM
5500
6000
6500
7000
7500
Time (s)
C
Response Units
39000
38500
38000
37500
Blank
0.625 µM
1.25 µM
2.5 µM
5 µM
10 µM
5500
6000
6500
7000
7500
Time (s)
D
Response Units
900
800
700
600
500
400
Blank
0.625 µM
1.25 µM
2.5 µM
5 µM
10 µM
5500
6000
6500
7000
7500
Time (s)

Figure 8. Surface Plasmon Resonance analysis of amyloid-β 42 binding to sphingomyelin on the HPA sensor chip. Sphingomyelin liposomes were injected over the HPA sensor chip surface (A) and bound to the chip. After the lipid surface had stabilized, BSA was injected over the lipid-coated and control surfaces, which showed binding to the control surface as seen in the reduction in the subtracted signal in (A). Aβ42 was injected over both the active lipid (B) and control (C) surfaces. Binding was seen to the active surface at concentrations of 5 and 10 μM, while the reference surface showed binding at 10 μM. The reference-subtracted curve (D) shows the relative binding to each surface, with the 5 μM injection showing the largest relative response on the lipid surface. Arrows indicate the beginning of each injection, with the Aβ42 concentration applied.

Lipid Binding of Amyloid β species

In order to assess the conditions for SPR experiments we first replicated previously performed experiments which assessed the binding of amyloid β to lipid surfaces (53). For our replication we used only sphingomyelin lipid surfaces, as these surfaces had shown the highest-magnitude responses in previous experiments. Initial experiments were carried out using a L1 sensor chip on the Biacore T200. The chip was coated with lipids by injecting unilaminar liposomes over the chip, which produced a binding response of approximately 6.000 response units (RU) relative to the uncoated reference surface (Figure 7). Stabilization of the surface with two injections of 10 mM sodium hydroxide did not lead to an appreciable loss of material from the sensor surface. Amyloid beta 1-42 was injected over both the control and reference surfaces and bound to the lipid-coated surface, however unspecific binding was also observed on the reference surface, and this nonspecific binding was greater in magnitude than the binding to the experimental lipid surface (Figure 7). In order to counteract this we attempted to block the sensor surface, using the recommended injection of 1 mg/mL BSA over both the lipid-coated and reference surfaces. The lipid surface again showed a robust binding of sphingomyelin to the surface, achieving approximately 6,000 response units of coverage. Stabilization of the surface with 10 mM sodium hydroxide resulted in a loss of approximately 500 response units from the lipid coated surface. BSA was injected over both the lipid-coated and reference surfaces and showed binding to both. The lipid surface showed approximately 500 RU of BSA binding, returning the coverage to the maximum achieved during the liposome injection. The reference surface binding response to BSA was approximately 2-fold the response seen on the experimental surface, showing 1.000 RU of coverage after injection of BSA. Injections of

amyloid beta 1-42 over the BSA-blocked experimental and control surfaces still exhibited nonspecific binding to the reference surface with a magnitude greater than that seen on the lipid surface.

In an attempt to reduce the nonspecific binding we changed from using the L1 sensor chip, which binds a lipids to a series of hydrophobic molecules covalently coupled to a dextran matrix, to the HPA sensor chip, where the hydrophobic coating is directly coupled to the gold surface of the sensor, in hopes that the reduced complexity of the HPA surface would present fewer opportunities for nonspecific binding (Figure 8). Repetition of the lipid capture to this surface again showed robust capture to the surface, however the total magnitude was reduced roughly twofold to 3000 RU. Stabilization of this surface with injections of sodium hydroxide led to a reduction of 500 RU, leaving a final stable surface composed of approximately 2500 RU of captured lipids. We then repeated the blocking phase by injecting BSA over both the lipid-coated experimental surface as well as the control surface, and once again observed a robust binding response to both surfaces. The magnitude of the binding response was once again larger on the uncoated control surface, and bound approximately 1500 RU of material, while the lipid coated surface bound approximately 500 RU of material. The subtracted trace showed that a similar amount of total mass was bound to both surfaces, and both surfaces were stable under normal running conditions. We then injected a dilution series of amyloid-β 1-42 over both surfaces. No binding was observed for concentrations of 0.625, 1.25, and 2.5 μM, however at a concentration of 5 μM binding was observed, and was greater on the lipid-coated surface compared to the BSA-blocked control. Binding was also observed at 10 μM, however at this concentration we observed more nonspecific binding to the BSA coated reference surface than to the lipid-coated active surface.

Discussion

In this thesis we have developed the tools required to gain a further understanding of the role that clusterin plays in the pathogenesis of Alzheimer Disease. We first produced and characterized a monoclonal anti-clusterin antibody, G7, which we then used to create an affinity chromatography column for the purification of HEK293-expressed clusterin. We were able to establish a method for the expression and purification of recombinant clusterin, providing a key tool for future investigations into the mechanisms behind clusterin's altered function in AD. Additionally, we verified both the identity of the recombinant protein, using tryptic fingerprinting and Western blotting, as well as the chaperone activity of our protein using a protein aggregation assay. In addition to the purification and verification of recombinant clusterin, we fine-tuned a technique to create a stable lipid surface for the investigation of clusterin's interactions with lipids, which had been singled out as a potential AD-related functional change by previous experiments in our lab. We also developed a non-interactive protein blocking protocol, providing an inert reference surface to serve as a control for these lipid-binding experiments.

Production and characterization of recombinant clusterin

We successfully adapted the method of Dabbs & Wilson (50) for the production of pure, chaperone active, recombinant clusterin. Traditional bacterial-based expression techniques are insufficient for producing clusterin since the protein is extensively post-translationally modified and these modifications, specifically the cleavage into α- and β-chains, seem to be important for the chaperone activity of the protein (54). The method used here circumvents these issues by using HEK293 cells, which contain the necessary cellular machinery to perform the proteolytic processing and glycosylation of the protein, as an expression system. In order to purify the protein from HEK293 cell cultures we first used an anti-clusterin affinity column which was prepared in-house from a monoclonal antibody we purified from hybridoma cultures.

The ability of this antibody to immunoprecipitate clusterin from cell culture media was verified with a small-scale immunoprecipitation, the product of which was analyzed with MALDI-MS and found to contain a peak within the range of previously reported apparent molecular weights for clusterin. In-source decay sequencing confirmed that the protein was clusterin, and the intact mass we obtained represents, to our knowledge, the first reported molecular weight of clusterin derived by a method other than gel electrophoresis.

Due to the low yield of antibody we obtained from the hybridoma cultures, the affinity column was prepared with the minimum viable concentration of antibody which is likely the current limiting factor on the yield of recombinant clusterin and may become problematic as the technique is scaled up. Further optimization of the hybridoma culture conditions and the creation of a new column with increased coupled antibody, increased volume of packing media, or both of these improvements will likely be required in the future in order to produce larger quantities of protein required for, by example, cell culture experiments in a timely fashion. After

initial purification with the affinity column, Western blotting and coomassie staining revealed that the majority of the material present was detected by anti-clusterin antibodies, however due to the presence of faint, high molecular weight bands which were observed via Coomassie stain but were not detected by Western blotting we elected to proceed with the cation exchange purification. In order to perform the cation exchange step we first needed to buffer exchange the affinity chromatography eluent from the 2M GdHCl elution buffer into a buffer which consisted of 20 mM MES at a pH of 6.0. While the original protocol used simple dialysis for this step we performed the buffer exchange using a series of desalting columns in order to reduce the time required for the purification process and to more quickly remove the GdHCl, a strong denaturing agent, from the product and thus reduce the chance of permanent alterations to the structure of purified clusterin.

After buffer exchange we completed the purification by loading the protein-containing fractions onto a cation exchange column. Since the pH of the running buffer used (6.0) is the same as the isoelectric point of clusterin we expected that the protein would be in an uncharged state and would therefore pass through the column. Since the majority of proteins have a pI greater than 6 (55) we expected that the majority of any contaminating proteins would bind to the column as they acquire a negative charge due to the pH of the solution being below their isoelectric point. When we performed the cation exchange step we instead observed no A280 peak in the flowthrough stage of the purification, indicating that all proteins present in the sample bound to the column. Elution by adding a 0.0 – 1.0 M sodium chloride gradient to the MES running buffer over 10 mL eluted a single A280 peak which, according to the theoretical model behind this purification step, consisted of clusterin as well as any impurities. Our assessment of the composition of the eluted peak using SDS-PAGE (in combination with

coomassie staining and Western blotting) and tryptic peptide mass fingerprinting found that the eluted peak from the cation exchange column produced a significant match for human clusterin and no other proteins. This indicates that any impurities which were present in the fraction loaded onto the cation exchange column bind with a much higher affinity to the column than the clusterin, as they did not elute from the column even at a concentration of 1 M sodium chloride while the clusterin eluted almost immediately. Analysis of the biological activity of our purified product showed that it was able to reduce the aggregation of BSA under mild reducing conditions by 40% compared to control levels, however the reduction was not as dramatic as had been obtained by Dabbs & Wilson.

One possible explanation for the difference in behavior between our adapted purification process and the original method used by Dabbs and Wilson is the formation of complexes between clusterin and other proteins in the cell culture media, particularly those from the FBS used to supplement the media. If these complexes were positively charged at pH 6.0 they would be expected to bind the cation exchange resin which is in agreement the elution profile we observed during our purification process. This possibility was of significant concern since the formation of such complexes could potentially impact the biological activity of the clusterin produced via our method and result in reduced chaperone activity of our purified clusterin relative to previously reported results. To test this hypothesis we purified clusterin from cells which were grown in standard HEK293 media without FBS supplementation in order to reduce the total protein amount in the cell culture media. When we purified clusterin from this serum-free media we observed the expected A280 peak in the flowthrough of the cation exchange column, indicating that clusterin grown in serum-containing media had formed a complex with FBS proteins, and that these complexes were the reason for the unexpected profile we had

previously seen. Testing this product using the aggregation assay showed no difference in chaperone activity between clusterin purified from serum-free media and that produced from serum-containing media, indicating that the complexes formed between clusterin and FBS proteins are either unstable and dissociate under the conditions of SDS-PAGE and the aggregation assay, thereby freeing clusterin to perform its anti-aggregation role, or that the existence of these complexes does not interfere with the ability of clusterin to chaperone other proteins.

Expansion of lipid-binding SPR techniques

We were also able to successfully expand on previously developed surface plasmon resonance techniques, providing the tools to further investigate the mechanisms of clusterin-lipid interactions and the mechanisms through which these might be altered. First, we verified the composition of the liposomes used in the preparation of the on-chip lipid surface by cryo-electron microscopy. Imaging the liposomes with this technique showed that extrusion produced a mostly homogenous population of unilaminar liposomes with diameters of 100 nm, which matched with our expectations.

In order to verify the functionality of the lipid surface we attempted to replicate previous results which investigated the lipid binding of amyloid-β. This led us to discover the need to block the reference sensor chip surface (i.e. the surface to which the lipids were not applied) with an inert protein, as the hydrophobic coating on the sensor chip surface proved capable of binding the peptides at higher levels than the lipid-coated active surface. This result can be readily explained, as amyloid-β is a highly hydrophobic molecule which is known to be very "sticky" and binds nonspecifically to many substrates (56).

Blocking the surface using BSA proved insufficient to prevent nonspecific binding of A**β** to the control surface so we changed from using the L1 sensor chip to the simpler HPA chip, which consists of a hydrophobic coating coupled directly to the gold surface of the sensor chip and does not include the intermediate dextran matrix found on the L1 sensor chip. Using the HPA sensor chip and the same capture/blocking protocol developed on the L1 chip we were able to replicate the previously performed experiments, showing concentration-dependent binding of A**β** to the lipid surface. Experiments using the same technique with recombinant clusterin in the

place of A**β** again produced an issue of nonspecific binding, however in this case the clusterin bound even to the blocking protein (BSA). Given the role of clusterin as a chaperone protein and its ability to bind promiscuously to other proteins, the occurrence of nonspecific binding is not surprising and our findings during the purification process indicate that clusterin is likely able to form complexes with proteins found in bovine serum (such as BSA). Despite this being normal behavior for clusterin, the nonspecific binding must be minimized in order to establish a reliable baseline against which we can compare our lipid-binding results.

Outlook

The work accomplished in this thesis sets the groundwork for further investigation into the role of clusterin in AD. By producing specific tools, developing methods, and characterizing both recombinant clusterin and the G7 antibody we have enabled a wide array of cell biology and biochemical experiments for future projects. For example, although clusterin has been shown to interact with amyloid-β and prevent the formation of both fibrils and low-n oligomers there have been no studies to date on the ability of clusterin to attenuate amyloid-β induced cell toxicity cells *in-vitro*. Having an in-house source of recombinant clusterin would enable this kind of experiment as it allows for another related avenue of research would be to see if clusterin promotes amyloid-β clearance.

In an effort to address the issue of nonspecific binding encountered while performing the SPR experiments outlined above we tried several alternative blocking agents with the goal of finding a protein which provided good coverage of the sensor chip surface, thus preventing nonspecific clusterin binding, without interacting directly with clusterin itself. Potential candidates included human insulin, lysozyme, and horse myoglobin. Of the screened candidates, preliminary tests pointed towards horse myoglobin as a preferable blocking agent since it showed good coverage of the sensor surface and no observable binding from the injection of clusterin over the surface. Additionally, the use of a horse protein helps to control for potential confounds which could arise by using a blocking agent which originates from the same species (human) as our eventual experimental material. Although promising, this preliminary finding still requires validation for use in conjunction with the lipid coating required for our experimental protocol.

Materials & Methods

General Chemicals

Unless otherwise specified, general laboratory chemicals and salts were ordered from Sigma Aldrich or Thermo Fisher

Fast-Performance Liquid Chromatography (FPLC)

All FPLC procedures (Pre-purification of FBS for antibody purification, antibody purification, affinity chromatography, on-column buffer exchange, cation exchange chromatography) were carried out using an AKTA Avant 25 (GE Healthcare)

Buffers

General lab buffering solutions were prepared as 10x stocks (25x for PBS), sterile filtered (0.22 μm) and stored in autoclaved bottles. The compositions of the stock solutions were as follows:

- **PBS:** 3.43M NaCl, 67.5mM KCl, 250 mM Na_2HPO_4 x 2 H_2O, 50 mM KH_2PO_4, pH 7.4-7.6
- **TBS:** 0.2 M Tris, 1.5 M NaCl, pH 7.6

Plasmids

The pRcCMV vector containing the CLU gene was provided to us by Mark Wilson (University of Wollongong). The plasmid sequence was verified by Sanger sequencing provided by McGill University and the Génome Québec Innovation Center.

Cell Culture Media

HEK293 Media consisted of Dulbecco's minimial essential medium (DMEM) supplemented with 10% fetal bovine serum (FBS), 2 mM glutamine, and 1 mM sodium pyruvate.

G7 hybridoma cells were cultured in DMEM supplemented with 10% FBS, 2 mM GlutaMAX, 1 mM sodium pyruvate, 10 mM HEPES, and 1x MEM nonessential amino acids solution. Media for hybridoma cultures was prepared fresh immediately before being added to the cells.

All cell culture media and supplements, as well as D-PBS and Trypsin/EDTA used for passaging cells were from Wisent Inc.

Consumables

All consumables (microfuge tubes, pipette tips, pipets, cell culture plates, ect.) were from Starsted and Thermo Fisher Scientific.

Eukaryotic Cell Culture:

All cell lines were incubated at 37°C with 5% CO_2 and 95% humidity. HEK293N cells were passaged before they reached 95% confluence. In order to passage cells they were washed once with PBS, detached using Trypsin/EDTA, and diluted 1:10 in fresh media. Cells were generally passaged into 10-cm dishes, various sized cell culture plates, or high-capacity flasks as required by the experiments which followed. To passage G7 hybridoma cells washing the plate with cell culture media proved to be sufficient to detach the cells, removing the need to wash the cells with PBS or to apply Trypsin/EDTA. Once detached, cells were either centrifuged at 500 RPM for 5 minutes in order to completely change the media or were simply diluted 1:5 in fresh media and seeded into 10-cm dishes.

Cell Stocks:

Eukaryotic cell lines were prepared for storage by trypsinizing fully confluent plates and centrifuging the cells at for 5 minutes at 500 RPM. Cells were then resuspended in cryo-storage media, which consisted of regular media for the cell type being frozen supplemented with 10% DMSO and an additional 10% FBS (typically bringing the final FBS concentration to 20%). Cells derived from a single plate were resuspended in 3 mL of cryo-storage media, which was then split into two cryogenic vials. The vials were immediately placed in a special storage container filled with isopropanol and left at -80°C for a minimum of 12 hours after which they were transferred to a liquid nitrogen freezer (-140°C) for long-term storage.

In order to thaw cells for use a vial of frozen cells was removed from the liquid nitrogen freezer and rapidly thawed using a 37^{o}C water bath. The cell suspension was added dropwise to 10 mL of cell culture media which was then centrifuged for 5 minutes at 500 RPM and replaced with fresh media to remove DMSO from the cells. The cells were then plated in two 5 cm dishes and allowed to recover for 24 hours, at which point the cells were trypsinized, seeded into 10 cm plates, and passaged normally.

Transfection of HEK293 cells:

Transfections were carried out when cells were 50-60% confluent using either polyethylenimine (PEI, Sigma-Aldrich), which was mixed at a 2:1 ratio with DNA in OptiMEM media (Gibco), vortexed gently, and left for 20-30 minutes to form complexes before being added to cells. The volume of transfection mixture used was equal to one-third the total media volume of the well, with the remaining two-thirds of the final media volume being made up with either fresh regular media or additional OptiMEM.

Cells were incubated with the transfection mixture for a maximum of 24 hours. After aspirating the transfection mixture cells were either harvested, transferred into fresh media, or transferred into selection media for the creation of stable cell lines.

Generation of HEK293 stable cell lines:

Stable cell lines were produced by first transfecting HEK293N cells, seeded in 6-well plates, using the standard transfection protocol. After transfection 1.5 mL of full media was added to each well and cells were allowed to grow for 24 hours before being passaged into 10 cm plates (one plate per well), with each plate containing 10 mL of full media. After 24h the media was changed to selection media containing the relevant selection antibiotic and cells were passaged normally, except that media was changed once every 48 hours at a minimum, regardless of confluence. Cell lines were deemed "stable" once passaged cells reached 90% confluence in approximately 48 hours with no detachment from the plate surface. Once stable, supernatant from the cells was collected and analyzed using SDS-PAGE + Western blot to verify the continued expression of the protein of interest. Cells were further amplified and prepared for storage using the standard storage protocol described above.

SDS-PAGE:

Samples were prepared for SDS-PAGE by mixing them with 6x gel loading buffer, which consisted of 25% Glycerol, 10% SDS, and 5% Bromophenol blue, then heating them for 10 minutes at 95^{o}C. Samples were loaded into an SDS-PAGE gel in an electrophoresis chamber (BioRad) containing tris-glycine running buffer (25 mM Tris, 190 mM glycine, 0.1% SDS). Gels were run at a constant current (30-35 mA per gel) until the desired separation was achieved and then either stained using the colloidal coomassie procedure to visualize total protein content or transferred to a nitrocellulose membrane for immunoblot detection of specific proteins of interest.

Western Blotting:

Proteins were transferred from SDS-PAGE gels to nitrocellulose membranes using either a semi-dry or wet transfer method. Semi-dry transfers were carried out using a TurboBlot apparatus (BioRad) for 10 minutes at 2.5A, while wet transfers were carried out using a transfer chamber (BioRad) in transfer buffer (25 mM Tris, 200 mM glycine, 10% v/v ethanol) for either 2 hours at 400 mA, or overnight at 200 mA. After transfer, membranes were blocked with 5% w/v BSA in PBS with 0.1% Tween-20 for one hour at room temperature and then incubated with primary antibody, diluted in blocking solution, overnight at 4 degrees. After primary incubation residual antibody was removed by three 10 minute washes in PBS and membranes were incubated with horseradish peroxidase-coupled secondary antibody at a dilution of 1:10,000 for 2 hours at room temperature. Membranes were imaged by covering the membrane with ECL reagent (900 μl 0.25 mg/mL Luminol in 0.1M Tris/HCl, pH 8.6 mixed with 100 μL 1.1mg/mL p-hydroxy coumaric acid in DMSO and 0.3 μl hydrogen peroxide) and the chemiluminescent signal was detected using an ImageQuant™ LAS500 (GE Healthcare Life Sciences)

Coomassie Staining

SDS-PAGE gels were stained using a mass-spectrometry compatible version of the Coomassie stain. After running the gel was first washed with demineralized water to remove trace amounts of gel running buffer and then fixed using a solution of 50% methanol, 10% acetic acid in ddH_2O for a minimum of one hour. Residual fixative solution was removed with five, 5-minute washes in demineralized water. The staining solution was prepared by mixing 20 mL of staining solution 'A' (40% ammonium sulfate, 8% v/v phosphoric acid) with 60 mL of deionized water and adding 20 mL of staining solution 'B' (0.05% w/v coomassie brilliant blue in methanol). The solution was immediately poured over the gel and covered to prevent evaporation of the methanol from the solution. Proteins were stained with gentle shaking of gels overnight, after which they were washed with deionized water to remove excess staining and scanned.

Preparation of hybridoma conditioning media

Purification of the G7 antibody first required pre-purification of FBS, as some components of FBS can bind to and saturate the protein G column used for antibody purification, causing major reductions in the purity and yield of the antibody. In order to prepare media for purification FBS was mixed with DMEM at a 1:1 ratio and pumped over a 5 mL HiTrap Protein G column (GE Healthcare) at a flowrate of 1 mL/minute. The flowthrough from this column was captured and used in the place of FBS (at 20% to make up for the dilution factor) to prepare the antibody harvest media.

Expression and Purification of G7 antibody

Hybridoma cell lines expressing the monoclonal G7 antibody were incubated with harvest media until the media started to visibly become more yellow (typically 2-3 days) at which point the media was harvested and kept on ice until purification, which typically happened immediately.

After media was sufficiently conditioned it was centrifuged at 1000 g for 10 minutes to pellet suspended cells and larger debris. The supernatant was then transferred to a fresh tube and centrifuged at 5700 g for 30 minutes to pellet smaller debris fragments. The supernatant was then filtered (0.22 μm) and kept on ice until loaded onto a 5 mL HiTrap protein G column (GE Healthcare). The column was equilibrated in PBS and the supernatant was pumped over the column at a flow rate of 1 mL/min to allow antibody to bind. The column was then washed with 25 mL of PBS and eluted with 10 mL of 100mM Glycine, pH 2.7. Immediately after elution the fractions containing the antibody were pooled and dialysed against three changes of PBS at 4^{o}C, concentrated to 1-2 mg/mL using a 10 kDa cutoff centrifuge filter (Amicon), and stored at -80^{o}C.

Immunoprecipitation with G7 antibody

Immunoprecipitation (IP) was performed by mixing 35 μL of protein G Sepharose beads (EMD Millipore) with 500 μL of supernatant from clusterin-expressing HEK293 cells, 20 μL of 50x protease inhibitor cocktail (Roche), 5 μl of 1.7 mg/mL purified G7 antibody, and 440 μL of PBS to bring the final reaction volume to 1 mL. This precipitation reaction was incubated overnight at 4 degrees, with end-over-end shaking then the beads were pelleted and the reaction mixture removed. The beads were then washed three times with 1 mL of PBS, two times with 300 μL of ammonium acetate and eluted by incubating with 350 μL of 50% acetic acid for 5 minutes at room temperature. This elution step was performed twice and the resulting fractions were combined before being dried using a Speed Vac and stored at -20 degrees until analysis.

MALDI-MS verification

Clusterin purified via immunoprecipitation was reconstituted in 30% acetonitrile, 70% 0.1% TFA (30/70 ACN/TFA) One μL of sample was mixed with 1 μL of DHB matrix solution then spotted in duplicate on a ground steel target plate and allowed to air dry. DHB matrix was prepared by sonicating a supersaturated solution of DHB in 30/70 ACN/TFA for 5 minutes, then centrifuging at 10,000 RPM for 5 minutes to pellet undissolved DHB. Mass spectra were gathered using an UltraflexExtreme TOF/TOF MALDI mass spectrometer (Bruker), with each final spectrum composed of five, 500-shot samples taken at 80% power.

Antibody Coupling

CNBr-activated Sepharose 4B (GE Healthcare) was used as the base column packing media for preparation of the immunoaffinity column.

Lyophilized Sepharose powder was weighed out and suspended in 1 mM HCl. The media was washed with 1 mM HCl for 15 minutes to remove packaging additives and then with 50 mL of coupling buffer to remove any traces of acid from the media. The ligand to be attached (in this case the g7 antibody) was dialysed against 2 changes of coupling buffer (100 mM sodium bicarbonate, 500 mM sodium chloride, pH 8.3) at 4^{o}C, adjusted to a concentration of 2 mg/mL and then combined with the washed Sepharose beads and incubated with end-over-end shaking at 4 degrees overnight . Following coupling, beads were blocked with 100 mM Tris HCl, pH 8.0, for one hour at room temperature and then washed three times with alternating 100 mM Tris pH 8.0, 500 mM sodium chloride and 100 mM acetic acid, 500 mM sodium chloride solutions before being transferred into PBS with 0.1% sodium azide for storage at 4^{o}C.

Immunoaffinity Column Preparation

The G7 affinity column was prepared by pouring antibody-bound Sepharose into a Tricorn 10/50 column (GE Healthcare). 5 mL of antibody-bound Sepharose beads were suspended in 10ml of PBS and poured into the 5 mL base column coupled to a 10mL column to contain the excess volume. The remaining space in the overflow column was filled with PBS and attached to an AKTA avant to pack the media. Packing of the media was accomplished by flowing PBS through the column at the maximum allowable flowrate of 1.0 mL/minute for 30 minutes. After initial packing the extra column was replaced by the upper connector and the media was packed again with PBS at a flowrate of 1 mL/min, then equilibrated with PBS+Az for storage at 4 degrees.

Clusterin Purification

Purification of clusterin was performed using a modified method adapted from Dabbs and Wilson (50). HEK293 cells stably transfected with clusterin were seeded in 10cm plates and allowed to grow to confluence (typically 2-3 days). Cells were then trypsinized and seeded into 75cc flasks where they were allowed to grow for 7-10 days. The supernatant was harvested from these flasks and centrifuged for 10 minutes at 1000 xg to pellet any detached cells or debris, then filtered through a 0.22 micron filter and kept on ice until applied to the affinity column.

Affinity Chromatography

The G7 affinity column was equilibrated in PBS and Clu-containing media was pumped over the column at a flowrate of 0.2 mL/min in order to allow the protein to bind the antibody. The column was then washed with 5 column volumes of PBS to remove residual media, followed by 5 column volumes of PBS with 0.05% Tween-20 in order to remove any lipids. Any nonspecifically bound proteins were eluted using a nonspecific elution buffer (200mM sodium acetate, 500 mM NaCl, pH 5.0) and finally clusterin was eluted using 2 M GdHCl in PBS. Fractions containing the A280 peak (typically two 2-mL fractions) of the elution were pooled and immediately buffer exchanged into "cation running buffer" (20 mM MES, pH 6.0) using a series of three 5 mL HiTrap desalting columns joined in series. The fractions containing the A280 peak from the buffer exchange step were then loaded onto a HiTrap SPXL cation exchange column equilibrated in cation running buffer at a flow rate of 0.5 mL/min, washed with two column volumes of cation running buffer and then eluted with a 0-1 M NaCL gradient. 100 ul aliquots of each fraction of interest were taken for analysis by SDS-PAGE and

Clusterin-containing fractions were pooled and concentrated using an amicon centrifugal filter system.

Peptide Mass Fingerprinting

A tryptic digest of eluent from the purification was carried out using a protocol that allowed proteins to first be visualized on an SDS-PAGE gel and then digested and analyzed using mass spectrometry. 30 μL of concentrated purified Clusterin (1 mg/mL) was loaded onto a precast 10-14% SDS-PAGE gel which was then stained using the standard colloidal Coomassie protocol. The gel was imaged and all stained protein bands were excised from the gel, chopped into cubes, and transferred to a microfuge tube. The gel fragments were dehydrated using alternating 80% ACN and 20 mM ammonium bicarbonate washes until the gel appeared white. Trypsin was prepared by diluting 10 μL of 1 μg/μL trypsin in 90 μL of 100 mM ammonium bicarbonate. One gel volume of diluted trypsin was added to the gel fragments and incubated for 30 minutes to allow the trypsin to penetrate the gel, after which another gel volume of 20 mM ammonium bicarbonate was added and the digest reaction was incubated at 4^{o}C overnight. The digest was stopped by adding one gel volume of 5% formic acid, and the reaction was then centrifuged at 1000 g for 5 minutes. The supernatant containing the peptides was transferred to a fresh microfuge tube, dried using a Speed Vac and stored at -20^{o}C until analyzed.

Aggregation assay

Chaperone activity was assessed by inducing BSA (1.5 mg/mL) to precipitate using 2 mM dithiothreitol (DTT) and incubating at 37^{o}C for 16 hours. Clusterin was added at a concentration of 0.3 mg/mL and ovalbumin (Novus Biologicals) was used as a non-chaperone active control at an equimolar ratio to the active Clusterin amount. The absorbance at 360 nm was continuously monitored using a Synergy H1 photometer (Biotek) as 360 nm light is sensitive to the formation of protein aggregates which cause light scattering and increased absorbance.

Liposome Preparation

All lipids were ordered from Avanti Polar Lipids and were provided dissolved in chloroform. Lipids were stored at -20^{o}C until used to prepare liposomes. Liposomes for SPR experiments were prepared from a lipid film, produced by evaporating the chloroform from the lipid solution under a stream of nitrogen gas. The film was dried under vacuum overnight then resuspended in PBS at 37^{o}C with glass beads (to improve mixing) and gentle shaking for 2 hours. Following resuspension the liposomes were sonicated for 10 minutes at 4^{o}C and then heated to 40 degrees in preparation for extrusion. Unilaminar liposomes were created using the Avanti mini-extruder. The extruder was prepared according to the manufacturer's instructions and heated to 40^{o}C. One syringe was filled with the rehydrated lipid solution and the liposomes were passed through the extruder 21 times then transferred to a microfuge tube. Liposomes were kept at 37^{o}C while being used in order to maintain the fluidity of the lipid membrane, and stored at 4^{o}C when not in use for a maximum of 3 days.

Preparation of the Lipid surface

The lipid surface for both sensor chips (L1 and HPA) was prepared by injecting a 1:30 dilution of extruded liposomes in PBS at a flow rate of 10 μL/min for 30 minutes. The surface was stabilized mechanically by raising the flowrate to 50 μL/min and then by the injection of two five-minute pulses of 10 mM sodium hydroxide.

Amyloid-β lipid binding

Lyophilized amyloid-β peptides were monomerized by resuspending the lyophilized peptide in 80% formic acid, at a concentration of 1 μg/μL. The formic-acid dissolved peptides were aliquoted into microfuge tubes and dried using a Speed Vac, then stored at -20^{o}C in a sealed container until use. Peptides for experiments were re-suspended to a concentration of 1 μg/μL by adding half the final volume of 1% ammonia, sonicating for 10 minutes at 4^{o}C, bringing the sample to the final volume with deionized water, and sonicating for another 10 minutes at 4^{o}C. The peptides were kept on ice until prepared for injection at which point they were diluted in PBS and injected at a flow rate of 10 μL/min for 5 minutes, followed by a 5 minutes long disassociation phase. Injections were all performed sequentially, as regeneration of the lipid surface required a full strip and recapture of the lipids and blocking protein.

Blocking of SPR reference surface

Blocking of the reference surface was achieved by injecting the blocking protein at a concentration of 1 mg/mL over the surface using a flowrate of 10 μL/min and a total injection time of 5 minutes. The protein surface was stabilized using the same protocol as for the lipid capture.

References

1. Alzheimer’s Associtation. Alzheimer’s Disease: What is Alzheimer's? (2017).
2. Brookmeyer, R., Johnson, E., Ziegler-Graham, K. & Arrighi, H. M. Forecasting the global burden of Alzheimer’s disease. *Alzheimer’s Dement.* **3,** 186–191 (2007).
3. Alzheimer’s Association. *2017 Alzheimer’s Disease Facts and Figures*. (2017).
4. Hardy, J. & Allsop, D. Amyloid deposition as the central event in the aetiology of Alzheimer’s disease. *Trends Pharmacol. Sci.* **12,** 383–388 (1991).
5. Binder, L. I., Guillozet-Bongaarts, A. L., Garcia-Sierra, F. & Berry, R. W. Tau, tangles, and Alzheimer’s disease. *Biochim. Biophys. Acta - Mol. Basis Dis.* **1739,** 216–223 (2005).
6. Annaert, W. & De Strooper, B. A Cell Biological Perspective on Alzheimer’s Disease. *Annu. Rev. Cell Dev. Biol.* **18,** 25–51 (2002).
7. Baglioni, S. *et al.* Prefibrillar Amyloid Aggregates Could Be Generic Toxins in Higher Organisms. *J. Neurosci.* **26,** 8160–8167 (2006).
8. Snyder, S. W. *et al.* Amyloid-beta aggregation: selective inhibition of aggregation in mixtures of amyloid with different chain lengths. *Biophys. J.* **67,** 1216–1228 (1994).
9. Pike, C. J., Burdick, D., Walencewicz, a J., Glabe, C. G. & Cotman, C. W. Neurodegeneration induced by beta-amyloid peptides in vitro: the role of peptide assembly state. *J. Neurosci.* **13,** 1676–1687 (1993).
10. Haass, C. *et al.* The Swedish mutation causes early-onset Alzheimer’s disease by β-secretase cleavage within the secretory pathway. *Nat. Med.* **1,** 1291–1296 (1995).
11. Tanzi, R. E. A genetic dichotomy model for the inheritance of Alzheimer’s disease and common age-related disorders. *J. Clin. Invest.* **104,** 1175–1179 (1999).
12. Rao, A. T., Degnan, A. J. & Levy, L. M. Genetics of Alzheimer disease. *Am. J. Neuroradiol.* **35,** 457–458 (2014).
13. Scheuner, D. *et al.* Secreted amyloid beta-protein similar to that in the senile plaques of Alzheimer’s disease is increased in vivo by the presenilin 1 and 2 and APP mutations linked to familial Alzheimer's disease. *Nat. Med.* **2,** 864–870 (1996).
14. Kehoe, P. *et al.* A full genome scan for late onset Alzheimer’s disease. *Hum Mol Genet* **8,** 237–245 (1999).
15. Zhang, S. *et al.* CLU rs9331888 Polymorphism Contributes to Alzheimer’s Disease Susceptibility in Caucasian But Not East Asian Populations. *Mol. Neurobiol.* **53,** 1446–1451 (2016).
16. Jenne, D. E. & Tschopp, J. Clusterin: the intriguing guises of a widely expressed glycoprotein. *Trends Biochem. Sci.* **17,** 154–159 (1992).
17. Fritz, I. B., Burdzy, K., Sétchell, B. & Blaschuk, O. Ram rete testis fluid contains a protein (clusterin) which influences cell-cell interactions in vitro. *Biol. Reprod.* **28,** 1173–1188 (1983).
18. Rosenberg, M. E. & Silkensen, J. Clusterin: Physiologic and pathophysiologic considerations. *Int. J. Biochem. Cell Biol.* **27,** 633–645 (1995).

19. Jenne, D. E. *et al.* Clusterin (complement lysis inhibitor) forms a high density lipoprotein complex with apolipoprotein A-I in human plasma. *J. Biol. Chem.* **266,** 11030–11036 (1991).
20. Yerbury, J. J., Stewart, E. M., Wyatt, A. R. & Wilson, M. R. Quality control of protein folding in extracellular space. *EMBO Rep.* **6,** 1131–6 (2005).
21. Jenne, D. E. & Tschopp, J. Molecular structure and functional characterization of a human complement cytolysis inhibitor found in blood and seminal plasma: identity to sulfated glycoprotein 2, a constituent of rat testis fluid. *Proc. Natl. Acad. Sci. U. S. A.* **86,** 7123–7127 (1989).
22. Hermo, L., Wright, J., Oko, R. & Morales, C. R. Role of epithelial cells of the male excurrent duct system of the rat in the endocytosis or secretion of sulfated glycoprotein-2 (clusterin). *Biol. Reprod.* **44,** 1113–1131 (1991).
23. Kim, N. *et al.* Human nuclear clusterin mediates apoptosis by interacting with Bcl-XL through C-terminal coiled coil domain. *J. Cell. Physiol.* **227,** 1157–1167 (2012).
24. Nuutinen, T., Suuronen, T., Kauppinen, A. & Salminen, A. Clusterin: A forgotten player in Alzheimer's disease. *Brain Res. Rev.* **61,** 89–104 (2009).
25. Leskov, K. S., Klokov, D. Y., Li, J., Kinsella, T. J. & Boothman, D. A. Synthesis and functional analyses of nuclear clusterin, a cell death protein. *J. Biol. Chem.* **278,** 11590–11600 (2003).
26. Kapron, J. T. *et al.* Identification and characterization of glycosylation sites in human serum clusterin. *Protein Sci.* **6,** 2120–33 (1997).
27. Bailey, R. W., Dunker, A. K., Brown, C. J., Garner, E. C. & Griswold, M. D. Clusterin, a binding protein with a molten globule-like region. *Biochemistry* **40,** 11828–11840 (2001).
28. Väkevä, A., Laurila, P. & Meri, S. Co-deposition of clusterin with the complement membrane attack complex in myocardial infarction. *Immunology* **80,** 177–82 (1993).
29. Saunders, J. R. *et al.* Clusterin depletion enhances immune glomerular injury in the isolated perfused kidney. *Kidney Int.* **45,** 817–827 (1994).
30. Murphy, B. F., Kirszbaum, L., Walker, I. D. & d'Apice, J. F. Sp-40,40, a newly identified normal human serum protein found in the SC5b-9 complex of complement and in the immune deposits in glomerulonephritis. *J. Clin. Invest.* **81,** 1858–1864 (1988).
31. Desikan, R. S. *et al.* The Role of Clusterin in Amyloid-β–Associated Neurodegeneration. *JAMA Neurol.* **71,** 180 (2014).
32. Wickner, S., Maurizi, M. R. & Gottesman, S. Posttranslational quality control: folding, refolding, and degrading proteins. *Sci. (New York, NY)* **286,** 1888–1893 (1999).
33. Feder, M. E. & Hofman, G. E. Heat-shock proteins, molecular chaperones, and the stress response: evolutionary and ecological physiology. *Annu Rev Physiol* **61,** 243–282 (1999).
34. Williams, D. B. Beyond lectins: the calnexin/calreticulin chaperone system of the endoplasmic reticulum. *J. Cell Sci.* **119,** 615–623 (2006).

35. Wyatt, A. R. *et al.* Clusterin facilitates in vivo clearance of extracellular misfolded proteins. *Cell. Mol. Life Sci.* **68,** 3919–3931 (2011).
36. Carver, J. A., Rekas, A., Thorn, D. C. & Wilson, M. R. Small Heat-shock Proteins and Clusterin: Intra- and Extracellular Molecular Chaperones with a Common Mechanism of Action and Function? *IUBMB Life* **55,** 661–668 (2003).
37. Li, X. *et al.* Clusterin in Alzheimer's disease: A player in the biological behavior of amyloid-beta. *Neurosci. Bull.* **30,** 162–168 (2014).
38. Yerbury, J. J. *et al.* The extracellular chaperone clusterin influences amyloid formation and toxicity by interacting with prefibrillar structures. *FASEB J.* **21,** 2312–22 (2007).
39. Beeg, M. *et al.* Clusterin binds to Aβ1-42 Oligomers with high affinity and interferes with peptide aggregation by inhibiting primary and secondary nucleation. *J. Biol. Chem.* **291,** 6958–6966 (2016).
40. Dabbs, R. A. & Wilson, M. R. Expression and purification of chaperone-active recombinant clusterin. *PLoS One* **9,** (2014).
41. Heller, A. R. *et al.* Clusterin protects the lung from leukocyte-induced injury. *SHOCK* **20,** 166–170 (2003).
42. Stewart, E. M. *et al.* Effects of glycosylation on the structure and function of the extracellular chaperone clusterin. *Biochemistry* **46,** 1412–1422 (2007).
43. Lakins, J. N. *et al.* Evidence that clusterin has discrete chaperone and ligand binding sites. *Biochemistry* **41,** 282–291 (2002).
44. Majari, T. M., Strasser, V., Nimpf, J. & Schneider, W. J. A model for modulation of leptin activity by association with clusterin. *FASEB J. Off. Publ. Fed. Am. Soc. Exp. Biol.* **17,** 1505–7 (2003).
45. Althoff, V. Untersuchungen zur Entstehung von Aβ-Peptiden und deren molekulare Wechselwirkungen mit Lipiden der zellulären Plasmamembran. (2013).
46. Weiller, G. F., Caraux, G. & Sylvester, N. The modal distribution of protein isoelectric points reflects amino acid properties rather than sequence evolution. *Proteomics* **4,** 943–949 (2004).